# Molecular iodine impairs chemoresistance mechanisms, enhances doxorubicin retention and induces downregulation of the CD44$^+$/CD24$^+$ and E-cadherin$^+$/vimentin$^+$ subpopulations in MCF-7 cells resistant to low doses of doxorubicin

ALEXANDER BONTEMPO[1], BRENDA UGALDE-VILLANUEVA[1], EVANGELINA DELGADO-GONZÁLEZ[1], ÁNGEL LUIS RODRÍGUEZ[2] and CARMEN ACEVES[1]

[1]Instituto de Neurobiología y [2]Centro de Física Aplicada y Tecnología Avanzada, Universidad Nacional Autónoma de México (UNAM), Campus Juriquilla, Juriquilla, Santiago de Querétaro 76230, Mexico

Received January 11, 2017; Accepted July 10, 2017

DOI: 10.3892/or.2017.5934

**Abstract.** One of the most dreaded clinical events for an oncology patient is resistance to treatment. Chemoresistance is a complex phenomenon based on alterations in apoptosis, the cell cycle and drug metabolism, and it correlates with the cancer stem cell phenotype and/or epithelial-mesenchymal transition. Molecular iodine ($I_2$) exerts an antitumor effect on different types of iodine-capturing neoplasms by its oxidant/antioxidant properties and formation of iodolipids. In the present study, wild-type breast carcinoma cells (MCF-7/W) were treated chronically with 10 nM doxorubicin (DOX) to establish a low-dose DOX-resistant mammary cancer model (MCF-7/D). MCF-7/D cells were established after 30 days of treatment when the culture showed a proliferation rate similar to that of MCF-7/W. These DOX-resistant cells also showed increases in p21, Bcl-2 and MDR-1 expression. Supplementation with 200 $\mu$M $I_2$ exerted similar effects in both cell lines: it decreased the proliferation rate by ~40%, and $I_2$ co-administration with DOX significantly increased the inhibitory effect (to ~60%) and also increased apoptosis (BAX/Bcl-2 index), principally by inhibiting Bcl-2 expression. The inhibition by $I_2$ + DOX was also accompanied by impaired MDR-1 induction as well as by a significant increase in PPARγ expression. All of these changes could be attributed to enhanced DOX retention and differential down-selection of CD44$^+$/CD24$^+$ and E-cadherin$^+$/vimentin$^+$ subpopulations. $I_2$ + DOX-selected cells showed a weak induction of xenografts in *Foxn1*$^{nu/nu}$ mice, indicating that the iodine supplements reversed the tumorogenic capacity of the MCF-7/D cells. In conclusion, $I_2$ is able to reduce the drug resistance and invasive capacity of mammary cancer cells exposed to DOX and represents an anti-chemoresistance agent with clinical potential.

*Correspondence to:* Dr Carmen Aceves, Instituto de Neurobiología, Universidad Nacional Autónoma de México (UNAM), Campus Juriquilla, Boulevard Juriquilla 3001, Juriquilla, Santiago de Querétaro 76230, Mexico
E-mail: caracev@unam.mx

*Key words:* molecular iodine, doxorubicin, MCF-7 cells, chemoresistance, xenografts

## Introduction

Breast cancer is one of the leading causes of death among women worldwide due mainly to its ability to metastasize and develop chemoresistance. It has been estimated that one-third of breast cancer patients relapse at some point and that 25% of all cases are resistant to therapy (1). Chemoresistance is complex and involves several cellular and molecular events including alterations in the cell cycle, apoptosis or DNA damage repair pathways and a greater capacity to excrete chemotherapeutic drugs (2). The cell cycle regulator p21, which historically has been considered as a suppressor protein in normal cells, was recently linked to cancer progression and chemoresistance (3). For instance, the Nrf2-p21 axis has been associated with an increase in the resistant tumor cell population, activation of antioxidant mechanisms and chemoresistance in MCF-7, MDA-MB-231 and T47D cells (4). Moreover, ErbB2-dependent overexpression of p21 correlates with resistance to the chemotherapeutic drug Taxol in breast cancer (5), suggesting that in pathological conditions this cell arrest mechanism is triggered to protect the tumor cells from toxic treatments commonly used to target DNA division and/or induction of apoptosis. In recent years, drug expulsion has been considered another key mechanism of chemoresistance. The ATP-binding cassette (ABC) transporter family with its 49 members present in the human genome is one of the largest and oldest known protein families (6). One feature common to all members of this family is that they are membrane transporters that, by consuming ATP, are able to expel from cells a wide spectrum of substrates, including vitamins, lipids, hormones, metabolic waste products and xenobiotics such as

toxins and drugs. Their expression and activity, in fact, are correlated with a decrease in the cytoplasmic concentration of drugs and consequent failure of therapy (7). In addition, in an analysis of cellular and population composition, the onset of chemoresistance has been linked to cancer stem cells (CSCs). CSCs are a cancer cell subpopulation that has been demonstrated to possess tumor-initiating properties and metastatic potential, and they are intrinsically chemoresistant (8). CSCs have been already described and characterized in several hematologic and solid tumors including breast cancer, where the $CD44^+/CD24^-$ surface marker profile has been considered a canonical CSC characteristic (9); although emerging evidence indicates that this profile is not exclusive to mammary cancer cells with CSC properties (10). Moreover, the origin of the CSC population is still controversial, and some other cellular events are associated with their stem-like profile as is the case for epithelial-mesenchymal transition (EMT). EMT in cancer is well documented and is characterized by a reversible conversion of cells with a polarized epithelial pattern into cells with a mesenchymal profile (11). At the molecular level, during EMT, epithelial cells lose adhesion molecules such as E-cadherin, lose their epithelial differentiation markers and acquire high motility by induction of vimentin and N-cadherin proteins. In fact, this transformation highly correlates with the $CD44^+/CD24^-$ profile and chemoresistance (12).

Several researchers have focused on improving chemotherapeutic treatment using natural molecules to limit chemoresistance and avoid significant increases in toxicity. Molecular iodine ($I_2$) is a chemical form of iodine that exerts significant antineoplastic effects on several types of cancer cells, and its actions could be mediated by multiple mechanisms. At moderately high concentrations, iodine induces a strong depolarization of mitochondrial membranes triggering mitochondrion-mediated apoptosis (13). Furthermore, $I_2$ is able to react with lipids and proteins producing several iodinated compounds. Among all the iodolipids 5-hydroxy-6-iodo-8,11,14,eicosatrienoic δ-lactone, also called 6-iodolactone (6-IL), has been confirmed to be an agonist of the peroxisome proliferator-activated receptor type γ (PPARγ). IL-6 promotes differentiation by decreasing the expression of specific markers associated with invasiveness and metastasis (14,15). Moreover, previous studies from our laboratory showed that when co-administered with doxorubicin (DOX), $I_2$ significantly improves conventional mammary cancer treatment in both women and rodents, and it diminishes the chemoresistance response (16,17). In the present study we developed a cell line resistant to low doses of DOX as a model to analyze in-depth how the $I_2$ supplement affects the chemoresistance response. DOX is an anthracycline antibiotic and is the most widely used chemotherapeutic drug in breast cancer treatment. Our results showed that after 30 days of exposure to 10 nM of DOX, MCF-7/D cells exhibited the same proliferation rate but higher expression of the p21, Bcl-2 and MDR-1 proteins associated with chemoresistance mechanisms in comparison with MCF-7/W. The molecular iodine supplement maintained its apoptotic effect in both types of cells, indicating that $I_2$ and DOX exert antineoplastic effects by different mechanisms. In addition, $I_2$ increased the intracellular retention of DOX and exerted a differential down-selection of the highly tumorigenic $CD44^+/CD24^+$ and $E\text{-}cad^+/vim^+$ subpopulations. The $I_2$ + DOX-selected cells showed a reserved tumorigenic competence in xenografts suggesting that the chemoresistance and invasive mechanisms were defective. All these $I_2$ actions were associated with a significant increase in PPARγ expression.

## Materials and methods

*Cell culture and $I_2$ + DOX treatment*. The MCF-7 cell line was obtained from the American Type Culture Collection (ATCC; Manassas, VA, USA) and cultured in Dulbecco's modified Eagle's medium (DMEM) (Gibco, Thermo Fisher Scientific, Grand Island, NY, USA) supplemented with 10% fetal bovine serum (FBS) and maintained at 37˚C in a 5% $CO_2$ atmosphere. Adriblastin® (Pfizer Inc., New York, NY, USA) was the source of DOX at a concentration of 35.4 ng/ml, equivalent to 10 nM DOX. The MCF-7/D cell line was generated by treating MCF-7/W cells for 30 days with 10 nM DOX. Both types of cells were authenticated follow the ATCC protocol by short tandem repeat analysis. Molecular iodine was prepared with 13 g of crystalline iodine (Macron-Avantor, Center Valley, PA, USA) and 60 g of potassium iodide (Sigma-Aldrich, St. Louis, MO, USA) in one liter of $ddH_2O$. The iodine concentration was confirmed by titration with a solution of 0.1 N sodium thiosulfate. A working concentration of 200 $\mu$M $I_2$ was employed in all assays.

*Proliferation assay*. Cells (25,000) were seeded into 6-well plates and left to recover for 24 h in DMEM before treatments. Medium and treatments were replaced daily before counting. Cell counting was performed using a Neubauer chamber. The coefficient of drug interaction (CDI) was calculated as reported by Gong *et al* (18) with the follow equation: CDI = ($I_2$ + DOX) x nt/($I_2$ x DOX), where ($I_2$ + DOX) is proliferation of the co-treated culture, nt is proliferation of the non-treated cells, while $I_2$ and DOX represent the proliferation of cultures treated with each alone. Values <0.7 are considered as synergic interaction; values in the range 0.7-1.3 indicate additive interaction, and values >1.3 indicate an inhibitory effect.

*RT-qPCR*. Total RNA was extracted using TRIzol® (Invitrogen, Carlsbad, CA, USA) as suggested by the manufacturer. Reverse transcription (RT) was performed using M-MLV Reverse Transcriptase (Promega Corp., Fitchburg, WI, USA) and antisense specific primers according to the manufacturer's protocol. Quantitative PCR was performed as follows: 0.5 $\mu$l of cDNA solution was added together with 0.4 $\mu$l 10 $\mu$M-specific primer mix (forward and reverse), 5 $\mu$l Maxima SYBR-Green/ROX qPCR Master Mix (Fermentas, Burlington, ON, Canada) and 4.1 $ddH_2O$. The reaction was performed using a Corbett research 3,000 rotor-gene. The thermal profile used was: 95˚C for 10 min as hot-start step followed by 35 repetitions of the amplification cycle (melting at 95˚C for 15 sec, annealing at 60˚C for 30 sec, elongation at 72˚C for 30 sec). Lastly, the melting curve was analyzed to check amplification specificity. Absolute gene quantifications were normalized to β-actin levels. Table I summarizes the primers used in the present study.

*Flow cytometry*. CD44 and CD24 staining was performed as follows. After a 72-h treatment, cells were washed with

Table I. Primer details.

| Gene name | Accession no. | Forward primer sequences | Reverse primer sequences | bp |
|---|---|---|---|---|
| ABCg2 | NM_001257386.1 | AGTGTTTCAGCCGTGGAACT | GCATCTGCCTTTGGCTTCAA | 194 |
| BAX | NM_001291428.1 | AAGCTGAGCGAGTGTCTCAAGCGC | TCCCGCCACAAAGATGGTCACG | 327 |
| Bcl-2 | NM_000633.2 | GTGGAGGAGCTCTTCAGGGA | AGGCACCCAGGGTGATGCAA | 306 |
| Survivin (Birc5) | NM_001168.2 | TTCTCAAGGACCACCGCATC | CCAAGTCTGGCTCGTTCTCA | 126 |
| E-cadherin | NM_004360.3 | TGCCCAGAAAATGAAAAAGG | GTGTATGTGGCAATGCGTTC | 200 |
| MDR-1 | NM_000927.4 | GAGAGATCCTCACCAAGCGG | ATCATTGGCGAGCCTGGTAG | 122 |
| p21 | NM_000389.4 | GACCATGTGGACCTGTCACT | GCGGATTAGGGCTTCCTCTT | 176 |
| Vimentin | NM_003380.3 | GAGAACTTTGCCGTTGAAGC | GCTTCCTGTAGGTGGCAATC | 163 |
| β-actin | NM_001101.3 | CCATCATGAAGTGTGACGTTG | ACAGAGTACTTGCGCTCAGGA | 175 |

Gene names and accession no., primer sequences and length of amplicon expressed as base pairs (bp).

phosphate-buffered saline (PBS) and detached with 0.05% EDTA/PBS. Cells (1-2x$10^6$) were incubated in PBS containing 0.05% EDTA + 0.05% BSA, and then for 1 h in ice with antibodies against CD24 (coupled to PE; diluted 1:50; Abcam, Cambridge, UK) and CD44 (coupled to FITC; diluted 1:50; BD Biosciences, San Jose, CA, USA). After a wash with PBS, cells were fixed using 2% formaldehyde in PBS for 10 min. After washing again with PBS, the cells were re-suspended with 1 ml PBS and analyzed.

Due to the cytoplasmic location of their epitope, E-cadherin (E-cad) and vimentin (vim) were stained as follows. After detaching using trypsin + 0.05% EDTA solution and washing with 0.05% EDTA/PBS, the cells were fixed with 2% formaldehyde in PBS for 10 min on ice. Cells were permeabilized using a 1:1 methanol/acetone solution at -20˚C for 1 min. After a PBS wash, the cells were incubated for 1 h on ice with antibodies to E-cad coupled to Alexa 647 (diluted 1:2,000) and to vim coupled to PE (diluted 1:20) (both from BD Biosciences). After a last PBS wash, cells were re-suspended in 1 ml PBS. A BD Biosciences Accuri C6 flow cytometer was used to analyze the population. VirtualGain® was applied to normalize background fluorescence among treatments. Data were acquired and visualized using BD Biosciences Accuri C6 software.

*DOX retention assay*. After a 72-h pretreatment with 200 $\mu$M $I_2$, cells were incubated with 20 or 500 nM DOX as follows. The medium was replaced with fresh DMEM, and the cells were incubated for 1 h. An appropriate volume of concentrated DOX was added directly to the culture, which was incubated for another 1.5 h. At this point the cells were detached with trypsin + 0.05% EDTA solution. A sample containing 1-2x$10^6$ cells was fixed with 2% formaldehyde in PBS. DOX fluorescence was detected by BD Biosciences Accuri C6 cytometer with excitation at 488 nM; emission filter 585/40. Data were acquired and visualized using BD Biosciences Accuri C6 software.

*Tumorogenic capacity*. Female athymic homozygotic (*Foxn1$^{nu/nu}$*, Harlan, Indianapolis, IN, USA) mice were housed in a temperature-controlled room (21±1˚C) with a 12-h/12-h light/dark schedule. They were given food (Purina certified rodent chow; Ralston Purina Co., St. Louis, MO, USA) and water *ad libitum*. All of the procedures followed the Animal Care and Use Program of the National Institutes of Health (NIH) (Bethesda, MD USA), and were approved by the Committee on Ethics in Investigation from INB (Protocol #035). When homozygotic animals were 6-weeks old, each animal was injected subcutaneously with 2x$10^6$ MCF-7/D cells in 50 $\mu$l PBS and 50 $\mu$l Matrigel. All animals were monitored daily for 20 days; any xenografts were detected and measured with an automatic Vernier, and their volume was calculated using the ellipsoid formula (19). On day 20, the presence of a tumor mass was corroborated by the use of a thermograph camera FLIR E40 (parameters are summarized in Table II), and digital processing software was implemented in MATLAB and FLIR Tools to calculate tumor temperature (MathWorks, Natick, MA, USA).

Table II. Camera parameters.

| | |
|---|---|
| Temperature range | -20 to 650˚C |
| Thermal sensitivity | <0.07 to 30˚C |
| Detector type | Focal plane array (FPA); uncooled microbolometer 160x120 pixels |
| Field of view | Focus 25˚ x 19˚ |
| Spectral range | 7.5-13 $\mu$m |

*Statistical analyses*. One- or two-way ANOVA was performed to determine the significance of differences between groups, followed by Tukey's test for the significance of differences among multiple experimental groups. DOX retention data were analyzed by Student's t-test. Tumor progression was calculated by linear regression analysis.

## Results

Initial characterization of the low-dose DOX-resistant model showed that at 10 nM DOX, the MCF-7/W cell culture maintained its proliferation rate at 60% of the untreated control, whereas 20 nM DOX induced a total block of proliferation at 96 h (Fig. 1A). The established DOX-resistant model required two and four times longer (8 and 14 days) to

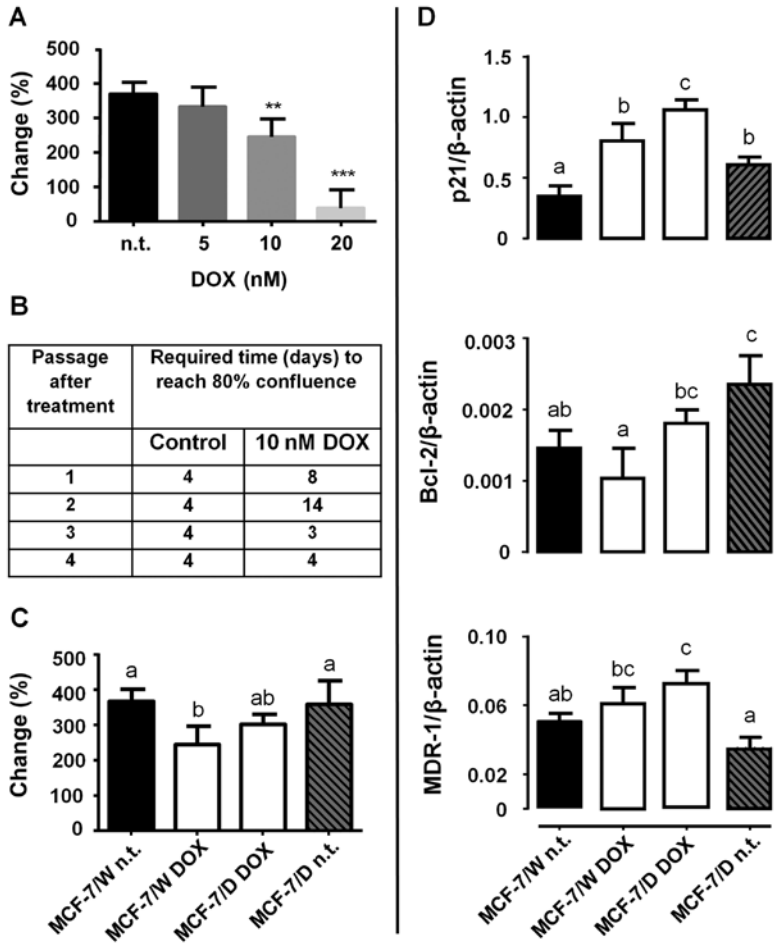


Figure 1. Doxorubicin (DOX)-resistant model characterization. (A) DOX dose-response after 96 h of treatment of wild-type MCF-7 cells (MCF-7/W). (B) Sub-selection of MCF-7/D cells. Time and passages required to reach 80% confluence in comparison with MCF-7/W (control). (C) Proliferation rate (% change) after 96 h of 10 nM DOX in wild-type (MCF-7/W) and DOX-resistant cells (MCF-7/D). (D) Gene expression after 72 h of treatment of p21 (cell cycle arrest), Bcl-2 (antiapoptotic) and MDR-1 (ABC membrane transporter) as measured by RT-qPCR; n.t., non-treated cells. Data are expressed as mean ± SD (n=3 independent assays); the asterisks indicate significant differences with respect to the control ($^{**}P<0.01$, $^{***}P<0.001$), and different letters indicate significant differences between groups ($P<0.05$).

reach 80% confluence after the first and second subcultures (passages), but within 30 days, the duplication rate had returned to the control value (Fig. 1B). The acute treatment (96 h) with 10 nM DOX decreased the proliferation rate (% change) only in MCF-7/W cells (Fig. 1C). DOX adaptation was accompanied by significant increases in the expression of the chemoresistance markers p21, Bcl-2 and MDR-1 (Fig. 1D, MCF-7/D DOX). Removal of chronic DOX treatment from MCF-7/D cells decreased p21 and MDR-1 expression (MCF-7/D n.t.).

Fig. 2 shows the effect of 200 $\mu$M $I_2$ alone or co-administered with 10 nM DOX. Iodine alone inhibited proliferation similarly in both types of cells, and the magnitude of this inhibition was also similar to that observed in the MCF-7/W cells treated with 10 nM DOX. Co-administration of $I_2$ + DOX exerted an additive effect on both cellular populations, as indicated by the coefficients of drug interaction (CDI). Gene analysis (Fig. 3) showed that the antineoplastic effect of $I_2$ *per se* was associated with a decrease in Bcl-2 and an increase in PPARγ expression in both the MCF-7/W and MCF-7/D cells. These effects were also observed with $I_2$ + DOX, but in this case $I_2$ also impaired cell cycle arrest (canceled the increase caused by DOX) and intensified the decrease in Bcl-2 expression, thereby enhancing apoptosis induction (BAX/Bcl-2 index). Survivin expression did not show any change.

Fig. 4 shows the effect of $I_2$ on the expression of two of the most important drug expulsion membrane transporters. Iodine did not modify the expression of MDR-1 in the MCF-7/W cells but blocked its induction by DOX in the MCF-7/D cells. In contrast, the $I_2$ supplement showed significant induction of ABCg2 transporter expression in all conditions (Fig. 4A). The DOX functional retention assay showed an increase in the intracellular concentration of DOX (fluorescence) when $I_2$ was administered for 72 h, with a tendency observed at low concentrations, but a clear and significant increase at 500 nM DOX (Fig. 4B).

Phenotypes of mammary CSCs (CD44/CD24) and the EMT process (E-cad/vim) were analyzed in MCF-7/D cells. Fig. 5 shows a significant decrease in the $CD44^+/CD24^+$ population in favor of the double-negative cell population in $I_2$-treated cells with and without DOX. The $CD44^+/CD24^-$ phenotype, which is the scarcest subtype (<4%) observed in these resistant cells, showed a modest but significant increase (6%) after $I_2$ treatment. Fig. 6 shows that in terms of EMT classification, the

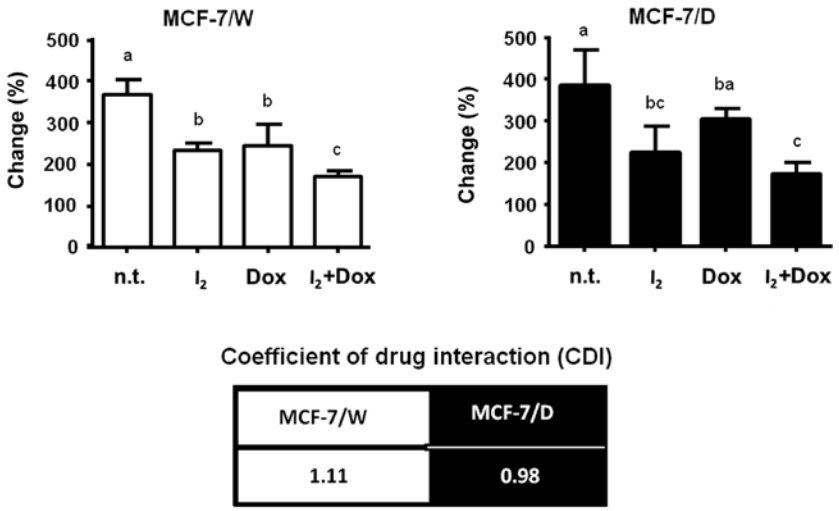


Figure 2. Proliferation assay. Cell count after 96 h of treatment with 200 $\mu$M $I_2$, 10 nM doxorubicin (DOX) and co-treatment ($I_2$ + DOX) of both cell lines. The coefficient of drug interaction (CDI) was calculated as described in the Materials and methods section. Data are expressed as mean ± SD (n=3 independent assays); different letters indicate significant differences between groups (P<0.05).

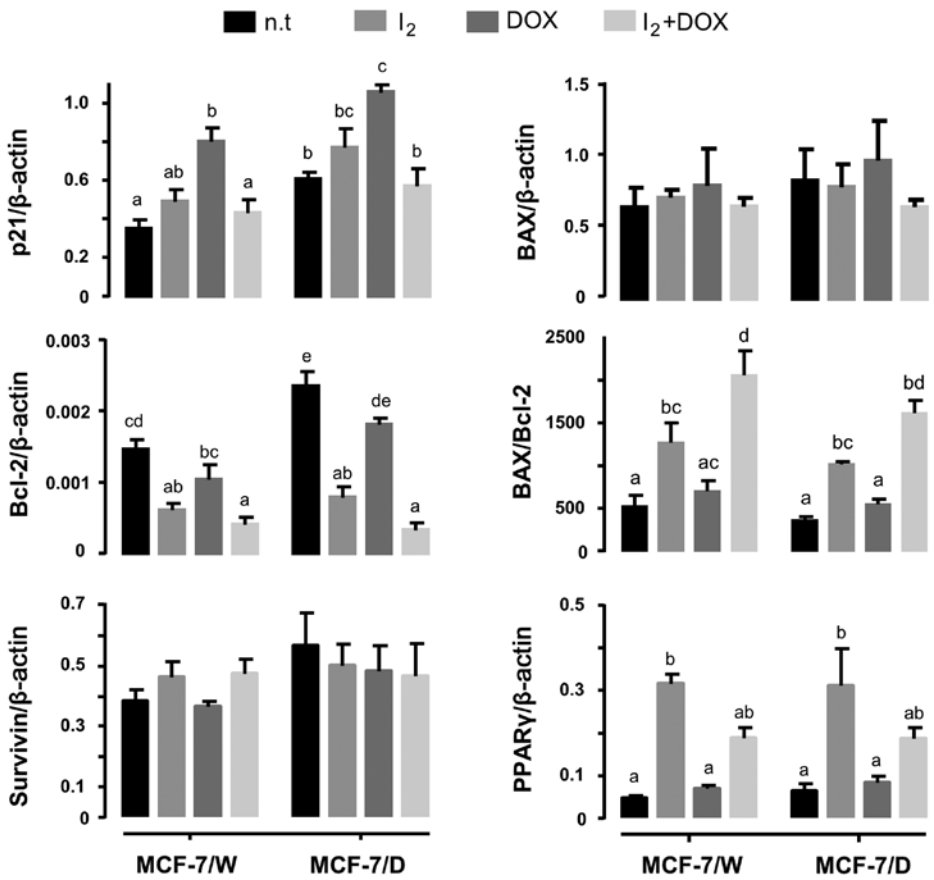


Figure 3. Gene expression. RT-qPCR analysis of genes related to cell cycle arrest (p21), apoptosis (BAX, Bcl-2 and survivin) and differentiation (PPARγ) after 72 h of treatment of both cell lines with 200 $\mu$M $I_2$, 10 nM doxorubicin (DOX) and the combination ($I_2$ + DOX). n.t., non-treated cells. Data are expressed as mean ± SD (n=3 independent assays); different letters indicate significant differences between groups (P<0.05).

most abundant population in the MCF-7/D cells corresponded to E-cad$^+$. Iodine treatment was accompanied by a significant decrease in E-cad$^+$/vim$^+$ in favor of E-cad$^+$/vim$^-$, and again, this was independent of DOX presence. RT-PCR analysis show that the $I_2$ supplement diminished vimentin expression (Fig. 6B).

To analyze the *in vivo* tumorigenic capacity of MCF-7/D subpopulations, athymic mice were inoculated with DOX-resistant cells pre-incubated for 96 h with 10 nM DOX (MCF-7/D) or 200 $\mu$M $I_2$ + 10 nM DOX (MCF-7/$I_2$ + D). Each animal was inoculated with both subpopulations on the left

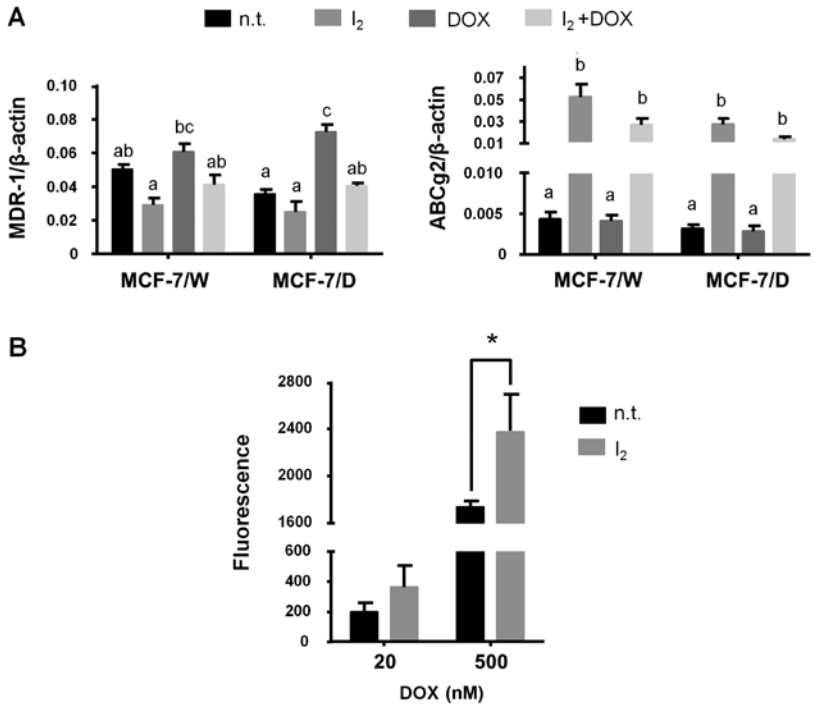


Figure 4. Expression and function of ABC transporter. (A) RT-qPCR analysis of MDR-1 and ABCg2 membrane transporter proteins after a 72-h incubation with 200 $\mu$M $I_2$, 10 nM doxorubicin (DOX) and the combination ($I_2$ + DOX) in both cell lines. (B) DOX intracellular retention measured by DOX fluorescence (Ex., 488 nm; Em. filter, 585/40) in non-treated (n.t.) or 200 $\mu$M $I_2$-treated MCF-7/D cells after exposure to 20 or 500 nM DOX for 1.5 h. Data are expressed as mean ± SD (n=3 independent assays); different letters indicate significant differences between groups (P<0.05), and asterisks indicate significant differences between the untreated control (P<0.05).

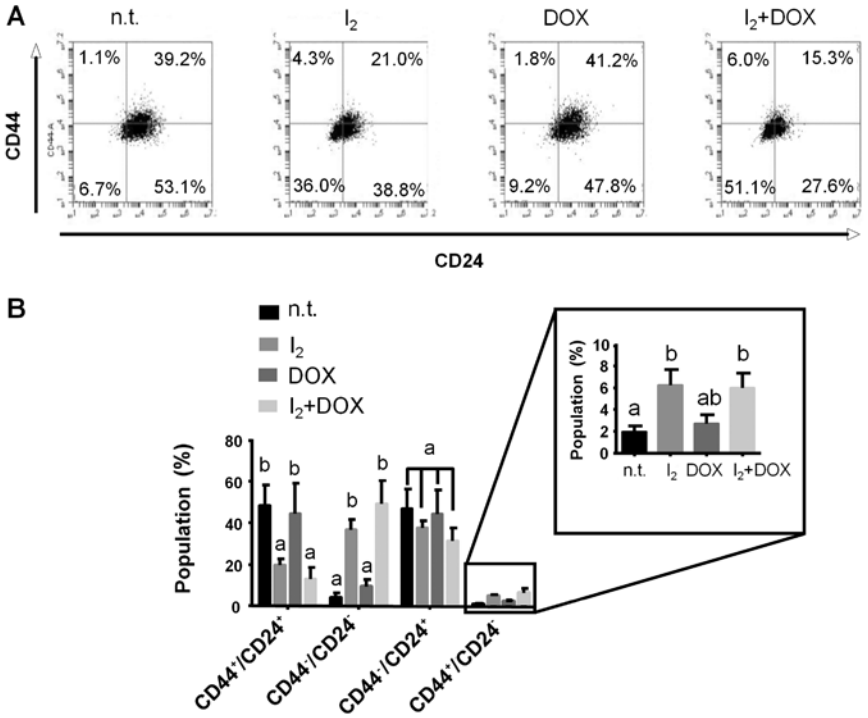


Figure 5. Cancer stem cell (CSC) subpopulation composition in MCF-7D cells. (A) Representative flow cytometric analysis of CSC markers (CD44 and CD24). (B) CSC subpopulation as a percentage of the total MCF-7/D cells after a 72-h treatment with 200 $\mu$M $I_2$, 10 nM doxorubicin (DOX) and the combination ($I_2$ + DOX). n.t., non-treated cells. Data are expressed as mean ± SD (n=3 independent assays); different letters indicate significant differences between groups (P<0.05).

or right side, respectively. Fig. 7 shows that MCF-7/D cells induced xenograft beginning on day 4 and maintained a rapid growth until day 12, whereas with MCF-7/$I_2$ + D, its growth rate and tumor size were significantly less.

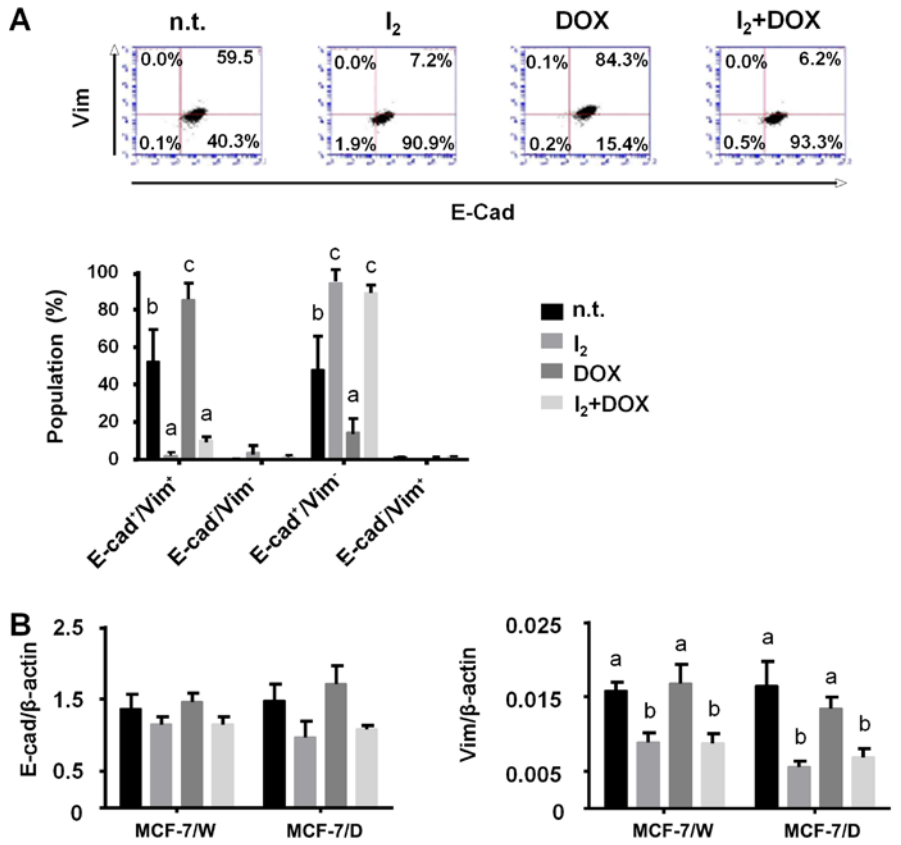


Figure 6. Characterization of MCF-7D cell subpopulations for EMT. (A) Representative flow cytometric analysis of EMT markers: E-cadherin (E-cad) and vimentin (vim); and percentage of subpopulations in the MCF-7/D culture after 72 h of treatment with 200 $\mu$M $I_2$, 10 nM doxorubicin (DOX) and combination ($I_2$ + DOX). (B) Gene expression (RT-qPCR) of E-cad and vim after 72 h of the same treatment. n.t., non-treated cells. Data are expressed as mean ± SD (n=3 independent assays); different letters indicate significant differences between groups (P<0.05).

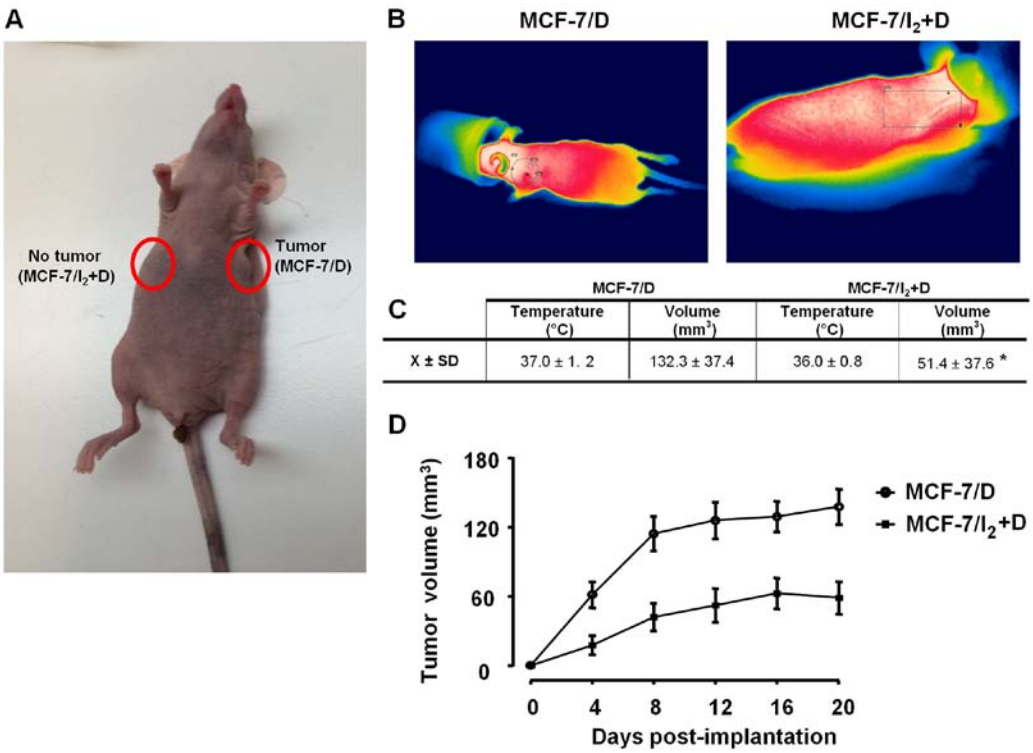


Figure 7. Xenograft generation and thermograph analysis of tumoral mass. Female athymic homozygotic (*Foxn1*$^{nu/nu}$) mice were inoculated with 2x10$^6$ DOX-resistant cells pre-incubated for 96 h with 10 nM doxorubicin (DOX) or the combination 200 $\mu$M $I_2$ + 10 nM DOX ($I_2$ + DOX). Each animal was inoculated with both subpopulations, on each side (n=6). (A) Image and (B and C) thermophotographs of nude mice. Circles indicate sites of xenografts in A. (D) Tumor volume growth of the xenograft tumors. Data are expressed as mean ± SD, and the asterisks indicate significant differences between groups (P<0.05).

## Discussion

The multistep protocol has been commonly used to establish *in vitro* models to study chemoresistance. Based on this method, resistant cells are selected by treating with a sequence of increasing DOX concentrations starting from low to over 1 mM depending on the author. However, in some cases this multi-step selection is accompanied by a loss of identity of cellular origin (20,21) or has only a weak correlation with clinical reality, where tumors undergo neither such step-by-step exposure nor such high DOX concentrations (22,23). For that reason, we used a single-step treatment extended for one month, a period that resembles the interval that separates one treatment cycle from the next. In our experience, DOX at a low concentration (10 nM) favors drug adaptation, as suggested by cell proliferation to a normal rate and decreasing sensitivity to DOX. At the molecular level, the antineoplastic effect of DOX results from a variety of actions; the best known are its ability to intercalate into DNA and to form a complex with topoisomerase II and DNA which triggers apoptosis, apparently via the p53-caspase pathway (24). In agreement, numerous studies indicate that DOX-resistant cells respond by decreasing topoisomerase II expression and increasing the expression of membrane drug transporters and the anti-apoptotic signal (22,25,26). Some of these mechanisms were observed in our MCF-7/D cells, such as cell cycle arrest (p21 upregulation), efficient drug expulsion (upregulated MDR-1 expression), and apoptosis evasion (BAX/Bcl-2 ratio decrease), indicating that these DOX-adapted cells can be considered as a chemoresistant cell model. The apparently paradoxical increase in p21 expression in response to DOX in both cell types agrees with recent studies showing that p21 can exert both anti- and pro-apoptotic effects in response to antitumor drugs, depending on cell type and cellular context (3). Cytotoxic drugs commonly act in mitotically active cells where they trigger apoptosis by inducing DNA damage (27). From this, it is reasonable to assume that early cellular alterations in reaction to such drugs may include apoptosis evasion and quiescence. Although the general observation that MCF-7/D cells return to the same proliferative rate as the wild-type, careful analysis reveals that these DOX-resistant cells include several subpopulations that could have different proliferation rates. Studies in our laboratory designed to confirm this hypothesis are now in progress.

The primary objective of the present study was to analyze for the first time the effect of iodine on the chemoresistance acquisition to DOX. Previous studies from our laboratory and others have shown that $I_2$ exerts antiproliferative and apoptotic effects in different models of cancer (16,17,28,29). Specifically, in mammary cell lines it has been demonstrated that cancerous (MCF-7, MDA-MB134, MDA-MB157 and MDA-MB436) and normal (MCF-10, MCF-12F) lines exhibit different sensitivity to $I_2$, but they all have a lower rate of proliferation when iodine is present (28,29). The most sensitive cell line is MCF-7, which is the focus of the present study as it represents the most frequent breast cancer in women (luminal, estrogen-positive) (30). Molecular iodine exerts a direct apoptotic effect by mitochondrial membrane depolarization and/or an indirect action via 6-iodolactone (6-IL). This iodolipid is generated by iodination of arachidonic acid; by activating PPARγ, 6-IL induces apoptosis and differentiation effects in MCF-7 cells (16,17). In the present study, $I_2$ maintained its apoptotic effect independent of the DOX-resistance mechanisms acquired by the cells. Several studies have shown that DOX-adaptation confers resistance to other drugs, due mainly to the overexpression of ABC transporters (22). It is possible that these membrane transporters cannot expel iodine. Indeed, our results showed that $I_2$ alone inhibited MDR-1 expression only weakly, but it significantly impaired MDR-1 upregulation by DOX treatment in MFC-7/D cells, suggesting that the changes associated with $I_2$ treatment were capable of interfering with the installation of DOX-resistance. One interesting observation is the significant increase in ABCg2 expression in both types of cells treated with $I_2$. It is well documented that PPARγ activation inversely modulates MDR-1 and ABCg2. Although the MDR-1 gene does not contain response elements to PPARs, these receptors can inhibit the Wnt/β-catenin pathway, which is directly involved in MDR-1 regulation (31). In contrast, ABCg2 is directly stimulated by PPARγ agonists (32) and although these transporters are overexpressed in some tumor types, they have also been detected in several normal tissues such as intestine, liver, brain, placenta and mammary glands (7). Moreover, this breast cancer resistance protein (ABCg2) is strongly induced in the mammary gland during pregnancy and lactation and is responsible for pumping vitamin B2 into milk, suggesting a physiological role in differentiated mammary cells (33). These facts, along with the observation that $I_2$ treatment is accompanied by significantly higher intracellular retention of DOX, suggest that the antineoplastic effect of iodine could be related to PPARγ activation resulting in maintaining drug sensitivity (downregulation of MDR-1 and, therefore, lower drug expulsion) and the induction of cell differentiation. It is well established that MCF-7 cells can respond to synthetic agonists of PPARγ by increasing lipid accumulation, terminating cell growth and undergoing changes characteristic of a less malignant state (14,34,35). These re-differentiation responses were also described by our group in mammary (MCF-12 and MCF-7), prostate (RWPE-1, LNCaP and DU-145) and neuroblastoma (SKN-AS and SKN-SH5Y) cell lines after $I_2$ or 6-IL administration (28,36,37). In this context, it is possible that the significant increase in the ABCg2 transporter corresponds more to an induction of differentiation than of chemoresistance. The analysis of CSC and EMT markers showed that the canonic CSC profile $CD44^+/CD24^-$ expected to be enriched in drug-resistant cells was poorly represented (<4%) in MCF-7/D cells, whereas the most abundant populations were the $CD44^+/CD24^+$ and $CD44^-/CD24^+$ subtypes (~40% each). The supplementation with $I_2$ showed a discrete increase in $CD44^+/CD24^-$ (~6%), no change in $CD44^-/CD24^+$ and a clear differential selection against $CD44^+/CD24^+$ with a significant increase in the double-negative population ($CD44^-/CD24^-$). Previous studies have described that the canonic $CD44^+/CD24^-$ profile is not the only profile that corresponds to an invasive phenotype. Indeed, in a recent study, using sphere-promoting (Mammocult; Stem Cell Technologies, Vancouver, BC, Canada) conditions, this double-positive subpopulation was found to be the most representative group in the MCF-7 CSC culture (30). Increases in the double-positive population were found to be associated with a worse outcome in salivary gland (38), pancreatic carcinomas (39), and in colorectal cancer this double-positive population represents the specific

marker for CSCs (40). Controversial results have been reported in relation to the $CD44^-/CD24^+$ profile. In various studies, increases in $CD24^+$ cells were found to be correlated with the most aggressive phenotype (41-43), whereas in others there was no correlation with prognosis (44,45). In contrast, the double-negative phenotype had no prognostic significance in breast cancer patients (45), and in preclinical studies these cells showed reduced capacity to induce tumor growth in soft agar and xenografts in mouse models (46), suggesting that these cells are less invasive. This less-aggressive profile found in $I_2$ + DOX cells was confirmed by the enrichment of $E\text{-}cad^+/vim^-$ cells. Indeed, the expected EMT profile ($E\text{-}cad^-/vim^+$) was absent in MCF-7/D cells, and the double-positive population was significantly diminished in favor of the $E\text{-}cad^+/vim^-$ subpopulation when these cells were treated with $I_2$. E-cadherin is a transmembrane glycoprotein involved in epithelial adherens junctions, and its loss could be sufficient to promote the invasion-metastasis cascade, activating specific downstream signal transduction pathways that bestow high motility on the cells by inducing vimentin and N-cadherin proteins (47). In contrast, vimentin which is the most commonly expressed and highly conserved member of the type III intermediate filament protein family is considered the main EMT marker. High vimentin expression is observed in several aggressive breast cancer cell lines. In MCF-7 cells, vimentin overexpression is accompanied by increases in motility and invasiveness. These characteristics were reduced by vimentin antisense oligos in MDA-MB-231 cells, which constitutively express this protein (48). Congruently, our results showed that $I_2$-treated cells exhibited the lowest vimentin expression and that the $I_2$ + DOX-treated subpopulation was powerless to initiate tumor xenografts, corroborating its weak invasive potential. The EMT process, which is triggered by factors such as transforming growth factor-β (TGF-β), SNAIL and TWIST, is reverted by PPARγ activation (49,50). Studies have shown the antineoplastic effects of PPARγ ligands in various preclinical models (51); however, agonists of these receptors used as monotherapy failed to exert therapeutic benefits in advanced stage breast patients (52). Notably, PPARγ agonists in combination with the conventional antineoplastic drugs, such as carboplatin or tumor necrosis factor-related apoptosis-inducing ligand (TRAIL), showed synergistic effects, indicating that differentiation induced by PPARγ activation restored sensitivity to the cytotoxic drug (53,54). These synergistic effects were replicated in cells treated with DOX + $I_2$ in both preclinical (16) and clinical studies (17), supporting the notion that some $I_2$ effects are mediated by PPARγ activation.

In conclusion, the use of molecular iodine at a moderately high concentration restored the sensitivity of mammary cancer cells MCF-7/D to DOX. Impaired DOX expulsion and decreased expression of the chemoresistance markers p21, Bcl-2 and MDR-1 resulted in the selection of a less aggressive population, suggesting the potential of $I_2$ as a clinically useful anti-chemoresistance agent.

## Acknowledgements

We thank M. Juana Cárdenas-Luna, Felipe Ortiz, Adriana González and Michael Jeziorski for technical assistance, Leonor Casanova and Lourdes Lara for academic support, Dorothy Pless for proofreading and Martin Garcia-Servín and Alejandra Castillo for animal care advice. We extend special thanks to Mario Nava-Villalba and Silvia Angulo Barbosa for their contributions to scientific discussions and to Guadalupe Delgado, who will live forever in our memories, for technical and academic assistance. The present study was partially supported by grants: PAPIIT-UNAM, IN201516. Alexander Bontempo is a graduate student of UNAM in the PhD Program in Biomedical Sciences of the National Autonomous University of Mexico (Programa de Doctorado en Ciencias Biomédicas, Universidad Nacional Autónoma de México) and received fellowship 262489 from CONACYT.

## References

1. Martin HL, Smith L and Tomlinson DC: Multidrug-resistant breast cancer: Current perspectives. Breast Cancer 6: 1-13, 2014.
2. Gong J, Jaiswal R, Mathys JM, Combes V, Grau GE and Bebawy M: Microparticles and their emerging role in cancer multidrug resistance. Cancer Treat Rev 38: 226-234, 2012.
3. Abbas T and Dutta A: p21 in cancer: Intricate networks and multiple activities. Nat Rev Cancer 9: 400-414, 2009.
4. Achuthan S, Santhoshkumar TR, Prabhakar J, Nair SA and Pillai MR: Drug-induced senescence generates chemoresistant stemlike cells with low reactive oxygen species. J Biol Chem 286: 37813-37829, 2011.
5. Hawthorne VS, Huang WC, Neal CL, Tseng LM, Hung MC and Yu D: ErbB2-mediated Src and signal transducer and activator of transcription 3 activation leads to transcriptional up-regulation of $p21^{Cip1}$ and chemoresistance in breast cancer cells. Mol Cancer Res 7: 592-600, 2009.
6. Vasiliou V, Vasiliou K and Nebert DW: Human ATP-binding cassette (ABC) transporter family. Hum Genomics 3: 281-290, 2009.
7. Liang Y, Li S and Chen L: The physiological role of drug transporters. Protein Cell 6: 334-350, 2015.
8. Abdullah LN and Chow EK: Mechanisms of chemoresistance in cancer stem cells. Clin Transl Med 2: 3-12, 2013.
9. Meyer MJ, Fleming JM, Lin AF, Hussnain SA, Ginsburg E and Vonderhaar BK: $CD44^{pos}CD49f^{hi}CD133/2^{hi}$ defines xenograft-initiating cells in estrogen receptor-negative breast cancer. Cancer Res 70: 4624-4633, 2010.
10. Bhat-Nakshatri P, Goswami CP, Badve S, Sledge GW Jr and Nakshatri H: Identification of FDA-approved drugs targeting breast cancer stem cells along with biomarkers of sensitivity. Sci Rep 3: 2530-2542, 2013.
11. May CD, Sphyris N, Evans KW, Werden SJ, Guo W and Mani SA: Epithelial-mesenchymal transition and cancer stem cells: A dangerously dynamic duo in breast cancer progression. Breast Cancer Res 13: 202-212, 2011.
12. Sarrio D, Franklin CK, Mackay A, Reis-Filho JS and Isacke CM: Epithelial and mesenchymal subpopulations within normal basal breast cell lines exhibit distinct stem cell/progenitor properties. Stem Cells 30: 292-303, 2012.
13. Shrivastava A, Tiwari M, Sinha RA, Kumar A, Balapure AK, Bajpai VK, Sharma R, Mitra K, Tandon A and Godbole MM: Molecular iodine induces caspase-independent apoptosis in human breast carcinoma cells involving the mitochondria-mediated pathway. J Biol Chem 281: 19762-19771, 2006.
14. Nuñez-Anita RE, Arroyo-Helguera O, Cajero-Juárez M, López-Bojorquez L and Aceves C: A complex between 6-iodolactone and the peroxisome proliferator-activated receptor type gamma may mediate the antineoplastic effect of iodine in mammary cancer. Prostaglandins Other Lipid Mediat 89: 34-42, 2009.
15. Nava-Villalba M, Nuñez-Anita RE, Bontempo A and Aceves C: Activation of peroxisome proliferator-activated receptor gamma is crucial for antitumoral effects of 6-iodolactone. Mol Cancer 14: 168-173, 2015.
16. Alfaro Y, Delgado G, Cárabez A, Anguiano B and Aceves C: Iodine and doxorubicin, a good combination for mammary cancer treatment: Antineoplastic adjuvancy, chemoresistance inhibition, and cardioprotection. Mol Cancer 12: 45-55, 2013.

17. Peralta G, Torres JM, Delgado G, Dominguez A, De Obaldía R, Duarte L, Paredes E, Avecilla C, Hernández S, Vega-Riverol L, *et al*: Iodine exhibits dual effects on breast cancer as a co-treatment with anthracyclines: Anti-neoplastic synergy and cardioprotector. In 102nd Annual Meeting, AACR, Orlando, FL, 2011. (abstract 3509). Cancer Res 71 (Suppl 8): 3509, 2011. doi: 10.1158/1538-7445.AM2011-3509.
18. Gong JH, Liu XJ, Shang BY, Chen SZ and Zhen YS: HERG $K^+$ channel related chemosensitivity to sparfloxacin in colon cancer cells. Oncol Rep 23: 1747-1756, 2010.
19. Thompson HJ: Methods for the induction of mammary carcinogenesis in the rat using either 7,12-dimethylbenz[a]antracene or 1-methyl-1-nitrosourea. In: Methods in Mammary Gland Biology and Breast Cancer Research. Ip M and Aschz BB (eds). 8th edition. Kluwer Academic/Plenum Publishers, NY, pp19-29, 2000.
20. Mehta K, Devarajan E, Chen J, Multani A and Pathak S: Multidrug-resistant MCF-7 cells: An identity crisis? J Natl Cancer Inst 94: 1652-1654, 2002.
21. Pirnia F, Breuleux M, Schneider E, Hochmeister M, Bates SE, Marti A, Hotz MA, Betticher DC and Borner MM: Uncertain identity of doxorubicin-resistant MCF-7 cell lines expressing mutated p53. J Natl Cancer Inst 92: 1535-1536, 2000.
22. Calcagno AM, Fostel JM, To KKW, Salcido CD, Martin SE, Chewning KJ, Wu CP, Varticovski L, Bates SE, Caplen NJ, *et al*: Single-step doxorubicin-selected cancer cells overexpress the ABCG2 drug transporter through epigenetic changes. Br J Cancer 98: 1515-1524, 2008.
23. Kars MD, Iseri OD, Gündüz U, Ural AU, Arpaci F and Molnár J: Development of rational in vitro models for drug resistance in breast cancer and modulation of MDR by selected compounds. Anticancer Res 26: 4559-4568, 2006.
24. Mehta K: High levels of transglutaminase expression in doxorubicin-resistant human breast carcinoma cells. Int J Cancer 58: 400-406, 1994.
25. Calcagno AM, Salcido CD, Gillet JP, Wu CP, Fostel JM, Mumau MD, Gottesman MM, Varticovski L and Ambudkar SV: Prolonged drug selection of breast cancer cells and enrichment of cancer stem cell characteristics. J Natl Cancer Inst 102: 1637-1652, 2010.
26. Järvinen TA, Tanner M, Rantanen V, Bärlund M, Borg A, Grénman S and Isola J: Amplification and deletion of topoisomerase IIalpha associate with ErbB-2 amplification and affect sensitivity to topoisomerase II inhibitor doxorubicin in breast cancer. Am J Pathol 156: 839-847, 2000.
27. AbuHammad S and Zihlif M: Gene expression alterations in doxorubicin resistant MCF7 breast cancer cell line. Genomics 101: 213-220, 2013.
28. Arroyo-Helguera O, Rojas E, Delgado G and Aceves C: Signaling pathways involved in the antiproliferative effect of molecular iodine in normal and tumoral breast cells: Evidence that 6-iodolactone mediates apoptotic effects. Endocr Relat Cancer 15: 1003-1011, 2008.
29. Rösner H, Torremante P, Möller W and Gärtner R: Antiproliferative/cytotoxic activity of molecular iodine and iodolactones in various human carcinoma cell lines. No interfering with EGF-signaling, but evidence for apoptosis. Exp Clin Endocrinol Diabetes 118: 410-419, 2010.
30. Smart CE, Morrison BJ, Saunus JM, Vargas AC, Keith P, Reid L, Wockner L, Askarian-Amiri M, Sarkar D, Simpson PT, *et al*: In vitro analysis of breast cancer cell line tumourspheres and primary human breast epithelia mammospheres demonstrates inter- and intrasphere heterogeneity. PLoS One 8: e64388, 2013.
31. Zhang H, Jing X, Wu X, Hu J, Zhang X, Wang X, Su P, Li W and Zhou G: Suppression of multidrug resistance by rosiglitazone treatment in human ovarian cancer cells through downregulation of FZD1 and MDR1 genes. Anticancer Drugs 26: 706-715, 2015.
32. Weiss J, Sauer A, Herzog M, Böger RH, Haefeli WE and Benndorf RA: Interaction of thiazolidinediones (glitazones) with the ATP-binding cassette transporters P-glycoprotein and breast cancer resistance protein. Pharmacology 84: 264-270, 2009.
33. van Herwaarden AE, Wagenaar E, Merino G, Jonker JW, Rosing H, Beijnen JH and Schinkel AH: Multidrug transporter ABCG2/breast cancer resistance protein secretes riboflavin (vitamin $B_2$) into milk. Mol Cell Biol 27: 1247-1253, 2007.
34. Ruiz-Vela A, Aguilar-Gallardo C, Martínez-Arroyo AM, Soriano-Navarro M, Ruiz V and Simón C: Specific unsaturated fatty acids enforce the transdifferentiation of human cancer cells toward adipocyte-like cells. Stem Cell Rev 7: 898-909, 2011.
35. Davies GF, Juurlink BH and Harkness TA: Troglitazone reverses the multiple drug resistance phenotype in cancer cells. Drug Des Devel Ther 3: 79-88, 2009.
36. Aranda N, Sosa S, Delgado G, Aceves C and Anguiano B: Uptake and antitumoral effects of iodine and 6-iodolactone in differentiated and undifferentiated human prostate cancer cell lines. Prostate 73: 31-41, 2013.
37. Núñez-Anita RE, Nava-Villalba M and Aceves C: Dose-dependent apoptotic effect of molecular iodine in two neuroblastoma cell lines. In: Possible Participation of Retinoic Acid Receptor. 14th International Thyroid Congress, Paris, France, Sept 2010. https://www.thyroid.org/professionals/meetings/past-meetings/14th-international-thyroid-congress/.
38. Soave DF, Oliveira da Costa JP, da Silveira GG, Ianez RC, de Oliveira LR, Lourenço SV and Ribeiro-Silva A: CD44/CD24 immunophenotypes on clinicopathologic features of salivary glands malignant neoplasms. Diagn Pathol 8: 29-40, 2013.
39. Ohara Y, Oda T, Sugano M, Hashimoto S, Enomoto T, Yamada K, Akashi Y, Miyamoto R, Kobayashi A, Fukunaga K, *et al*: Histological and prognostic importance of $CD44^+/CD24^+/EpCAM^+$ expression in clinical pancreatic cancer. Cancer Sci 104: 1127-1134, 2013.
40. Yeung TM, Gandhi SC, Wilding JL, Muschel R and Bodmer WF: Cancer stem cells from colorectal cancer-derived cell lines. Proc Natl Acad Sci USA 107: 3722-3727, 2010.
41. Kristiansen G, Winzer KJ, Mayordomo E, Bellach J, Schlüns K, Denkert C, Dahl E, Pilarsky C, Altevogt P, Guski H, *et al*: CD24 expression is a new prognostic marker in breast cancer. Clin Cancer Res 9: 4906-4913, 2003.
42. Bretz N, Noske A, Keller S, Erbe-Hofmann N, Schlange T, Salnikov AV, Moldenhauer G, Kristiansen G and Altevogt P: CD24 promotes tumor cell invasion by suppressing tissue factor pathway inhibitor-2 (TFPI-2) in a c-Src-dependent fashion. Clin Exp Metastasis 29: 27-38, 2012.
43. Ma ZL, Chen YP, Song JL and Wang YQ: Knockdown of CD24 inhibits proliferation, invasion and sensitizes breast cancer MCF-7 cells to tamoxifen in vitro. Eur Rev Med Pharmacol Sci 19: 2394-2399, 2015.
44. Mylona E, Giannopoulou I, Fasomytakis E, Nomikos A, Magkou C, Bakarakos P and Nakopoulou L: The clinicopathologic and prognostic significance of $CD44^+/CD24^{-/low}$ and $CD44^-/CD24^+$ tumor cells in invasive breast carcinomas. Hum Pathol 39: 1096-1102, 2008.
45. Chen Y, Song J, Jiang Y, Yu C and Ma Z: Predictive value of CD44 and CD24 for prognosis and chemotherapy response in invasive breast ductal carcinoma. Int J Clin Exp Pathol 8: 11287-11295, 2015.
46. Shen YA, Wei YH, Chen YJ: High CD44/CD24 expressive cells presented cancer stem cell characteristics and undergo mitochondrial resetting and metabolic shift in nasopharyngeal carcinoma. Cancer Res 71 (Suppl 8): Abstract nr 482, 2011.
47. Onder TT, Gupta PB, Mani SA, Yang J, Lander ES and Weinberg RA: Loss of E-cadherin promotes metastasis via multiple downstream transcriptional pathways. Cancer Res 68: 3645-3654, 2008.
48. Satelli A and Li S: Vimentin in cancer and its potential as a molecular target for cancer therapy. Cell Mol Life Sci 68: 3033-3046, 2011.
49. Tan X, Dagher H, Hutton CA and Bourke JE: Effects of PPARγ ligands on TGF-β1-induced epithelial-mesenchymal transition in alveolar epithelial cells. Respir Res 11: 21-33, 2010.
50. Reka AK, Kurapati H, Narala VR, Bommer G, Chen J, Standiford TJ and Keshamouni VG: Peroxisome proliferator-activated receptor-γ activation inhibits tumor metastasis by antagonizing Smad3-mediated epithelial-mesenchymal transition. Mol Cancer Ther 9: 3221-3232, 2010.
51. Elrod HA and Sun SY: PPARgamma and apoptosis in cancer. PPAR Res 2008: 704165, 2008.
52. Burstein HJ, Demetri GD, Mueller E, Sarraf P, Spiegelman BM and Winer EP: Use of the peroxisome proliferator-activated receptor (PPAR) gamma ligand troglitazone as treatment for refractory breast cancer: A phase II study. Breast Cancer Res Treat 79: 391-397, 2003.
53. Girnun GD, Chen L, Silvaggi J, Drapkin R, Chirieac LR, Padera RF, Upadhyay R, Vafai SB, Weissleder R, Mahmood U, *et al*: Regression of drug-resistant lung cancer by the combination of rosiglitazone and carboplatin. Clin Cancer Res 14: 6478-6486, 2008.
54. Bräutigam K, Biernath-Wüpping J, Bauerschlag DO, von Kaisenberg CS, Jonat W, Maass N, Arnold N and Meinhold-Heerlein I: Combined treatment with TRAIL and PPARγ ligands overcomes chemoresistance of ovarian cancer cell lines. J Cancer Res Clin Oncol 137: 875-886, 2011.